JOURNAL OF AERONAUTICAL MATERIALS
ISSN: 1005-5053

Vol. 43, Issue-01, 2023
pp. 890-905

ANALYSIS OF END LOSS AND ITS COMPENSATION IN SMALLER PARABOLIC TROUGHS: A COMPREHENSIVE STUDY

Lovebrat Saxena[a], Anil Kumar[b,c] and Archana Soni[a]

[a]Energy Centre, Maulana Azad National Institute of Technology, Bhopal -462 003 (India)

[b]Department of Mechanical Engineering, Delhi Technological University, Delhi -110 042 (India)

[c]Centre for Energy and Environment, Delhi Technological University, Delhi -110042 (India)

Abstract

Parabolic trough collector (PTC) based concentrated solar power (CSP) systems for industrial process heat (IPH) are small size systems due to space constraints and lower temperature requirements. These system uses solar radiations to heat thermal fluid, which transports heat to process applications. End loss in line concentrating systems is proportionally greater in smaller troughs as compared to larger trough systems. To quantify end loss, a multi-variate numerical model was studied in the present work. In this study, optics of a PTC has been numerically estimated and experimentally validated, focusing on end loss. End losses are observed 5% for less than 280 incidence angles and also they are limited to 15% between 280 and 600 incidence angles. However, end loss increases exponentially for greater than 600 incidence angles. Uncertainty in skipped length measurements is found 2.3%. Whereas propagation of uncertainty in the calculation of end loss factor was found to be 4.15%. Estimating end loss forehand to installation will enable a designer to select a site-specific design to minimize the end loss and enhance the heat collection through the system.

Keywords: Parabolic trough collector; Optical analysis; End loss analysis; Skipped length

1. Introduction

21st century is surrounded by significant threats like global warming, climate change, pollution and depletion of fossil fuels, etc., which adversely impact environment and human life. The scientific community is developing new and sustainable ways to tackle the threats arising from increasing energy demands amid the energy crisis without degrading the environment (E. Xu et al., 2015). The usability of renewable energy in transportation, domestic and industrial applications is proven as the best alternative to fossil fuel based energy for sustainable development. Among all renewable sources, solar energy is a vast, clean, economical, convenient, and safer source of energy, overcoming its diluted nature. It has proven itself as a potential alternative to conventional energy, to deal with the environmental problems like CO2 emission, energy crisis and climate change (Luo et al., 2015). According to an estimate, the amount of solar energy received annually is twice the energy obtained from all the fossil based energy sources combined, shows the vast availability of the energy resource (Hermann, 2006). Practically, solar energy is an abundant source of energy with a vast potential (Zhu et al., 2019). An investigation to assess the capability of power producing limit of CSP in Libya shows that CSP innovation is techno-monetarily practical in Libya (Belgasim et al., 2018). Islam et al. carried out an investigation on techno-financial aspects of different CSP advancements, and inferred that PTC and ST plants were most appropriate for the considered Malaysian locales

(Islam et al., 2019). The techno-economic impact of design changes in TES (Thermal Energy System) was studied and it was reported that type of storage tank used greatly affects cost of system (Andika et al., 2017). Purohit and Purohit examined the techno-monetary plausibility of CSP in India. CSP technology is fairly feasible in India and monetarily, north-western piece of India (Rajasthan and Gujarat) (Purohit & Purohit, 2010).

Fig. 1. Classification of CSP

Most of the research work has been done for analysis and performance of PTC, including simulations and experimental investigations, whereas end loss is a subject kept less addressed. End loss depends upon the angle of incidence and is independent of length of trough. Therefore, for high solar radiation collection, it becomes insignificant. In a smaller trough, specifically used in industrial applications, end loss plays a significant role. Considering the importance of endloss in the overall efficiency of PTC, a detailed analysis of endloss and investigation of its compensation techniques were required. On the other hand, much literature is available on thermal models of a PTC and their characteristics, as discussed by (Al-Sulaiman et al., 2015; de Oliveira Siqueira et al., 2014; S. A. Kalogirou, 2012; Lu et al., 2013; Nolte et al., 2015; Salgado Conrado et al., 2017; Sun et al., 2015).

Optical losses in PTC collectors during receipt of solar energy and conversion process are less addressed. End loss and cosine effect combinedly hold the maximum share in losses. An investigation on the seasonal effect of endloss with compensation suggests 20% increment in the instantaneous efficiency of LFR (Ma & Chang, 2018). Relative end loss formulation is done and results were compared for linear Fresnel reflector (LFR) and parabolic trough collector. Annual optical efficiency values for PTC and LFR were 58% and 43% with ECOSTAR approach and 57% and 43% with COLSIM approach (Morin et al., 2012). Theoretical and experimental analysis for examining the effect of end loss with and without a heat insulator and a coil heater was performed for a 50MW PTS in China (Lei et al., 2013). Optical analysis for arbitrary oriented and short PTC is also addressed with the three compensation techniques (Li et al., 2015; Zou et al., 2016). Diameter of HTF receiver should be chosen, considering the aperture width of the trough. Small diameter receiver with high aperture width trough suffers larger endloss at a constant incident angle. Hence, sunshade largely affects the performance of PTC and should be considered in practice (Zou et al., 2017). A new design with a rotatable axis is presented with an emphasis on end losses and cosine loses. Results were compared with a traditional single-axis system (Peng et al., 2013). Compensation of endloss in LFR using extended receiver, displaced receiver and their combination yields 50.3%, 20.2% and 48.7% enhancement in the yearly performance. Study suggests the use of extended receiver compensation techniques over other techniques (Bellos et al., 2019).

The objective of this study is to develop a mathematical model for assessing end losses for a parabolic trough placed at any inclination, location, date and time. The findings of numerical simulation based on a developed mathematical model have been validated with experimental observations. Experimentation was carried out on an indoor setup of the scaled-down model of Poly Trough 1800. The developed model is useful for researchers designing PTC based CSP systems for process heat applications.

2. Mathematical formulation of end loss

The problem consists of a PTC, a receiver and incoming beam radiations from the sun. Solar radiations falling on the surface of the collector are reflected and intercepting the receiver. Problem consists of multiple variables that have direct or indirect relation with the objective function, hence for simplification following set of assumptions were taken into consideration.

- For optical analysis, the reflector surface is considered to be smooth.
- Reflection coefficient is taken to be unity.
- Only beam radiations are taken into consideration; hence rays striking at the critical points of the trough are assumed parallel to each other.
- Single ray is used to derive the expressions.
- Since the parabolic trough employs single-axis tracking, thus facing the sun directly all the time.
- Real time tracking is assumed.
- Deflection of radiations from the sharp edges is not considered.

Physical factors are shown in Table 1 affect the amount of end loss occurring in a parabolic trough at any instant of time. Their dependency and ranges are also illustrated in tabular form.

Table 1- Characteristics of quantities affecting end loss

Declination angle (δ) and the angle of incidence (θ) are not independent variables. However, for the simplicity of expression, these are used and calculated separately.

Fig. 2. Schematic diagram for parabolic trough

Side view of a parabolic trough in Fig. 2. depicts the solar radiation falling at an angle, θ. Solar radiation falling on point A gets reflected and strikes the Heat Collecting Element (HCE) at point C. As per trigonometry, the relation between focal length (x) and skip length (d/2) can be expressed as:

$$\frac{d}{2} = x\,Tan\,\theta \qquad (1)$$

Skip length is considered d/2 to reduce the complexity of equations.

Aperture length of the trough, which contributes the thermal energy to heat transfer fluid, can be calculated as:

$$Sin(90-\theta) = \frac{y}{\left(l-\frac{d}{2}\right)}$$

$$y = \left(l - \frac{d}{2}\right) Cos\,\theta \qquad (2)$$

In a Parabolic Trough, the reflected radiation that does not concentrate over the receiver accounts for end loss. Length of trough participating in end loss depends upon the angle at which radiation is falling over the trough surface.

From properties of similar triangles ΔAEF and ΔAGD, the aperture length of collector involved in end loss can be expressed as:

$$z = y\left(\frac{d}{2l-d}\right) = \frac{d}{2}cos\,\theta \qquad (3)$$

Aperture area of the collector (Ael,ap) is responsible for end loss. It is obtained with the product of ineffective collector length (z) from Eq. (3) and the aperture width (w) of the parabolic trough and expressed as:

$$A_{el,ap} = w\left(\frac{d}{2}\right) Cos\,\theta \qquad (4)$$

Fraction of collector area involves in instantaneous end loss phenomenon, which is represented as the ratio of end loss aperture area to the total aperture area of the trough, is given as end loss factor:

$$\mu = \frac{\left\{\frac{d}{2} * \cos\theta\right\}}{z+y} \quad (5)$$

'd' is a dependent variable and it is a function of theta, whereas l is a constant for a trough under consideration.

Although angle of incidence (θ) can be directly measured, while in the case of a comprehensive model of end loss for any arbitrary set of condition, θ can be calculated if the given set of parameters in Table 2 are known (Duffie & Beckman, 2013; Tiwari & Tiwari, 2017).

$$Cos\,\theta = Sin\,L\,Sin\,\delta\,Cos\,\beta - Cos\,L\,Sin\,\delta\,Sin\,\beta\,Cos\,a_s + Cos\,L\,Cos\,\delta\,Cos\,\omega\,Cos\,\beta + Sin\,L\,Cos\,\delta\,Cos\,\omega\,Sin\,\beta\,Cos\,a_s + Cos\,\delta\,Sin\,\omega\,Sin\,\beta\,Sin\,a_s \quad (6)$$

For parabolic trough systems, the angle between the aperture surface and the horizontal plane β is generally kept 00. It is to avoid the formation of long shadows when the sun is at a lower altitude. Collector should be oriented in N-S orientation to collect maximum solar radiation. Hence, the surface azimuth angle (as) will become 00. Expression of incidence angle in Eq. (8). is reduced to (R. Xu & Wiesner, 2015):

$$Cos\,\theta = Sin\,L\,Sin\,\delta + Cos\,L\,Cos\,\delta\,Cos\,\omega$$

$$\theta = \cos^{-1}(Sin\,L\,Sin\,\delta + Cos\,L\,Cos\,\delta\,Cos\,\omega) \quad (7)$$

Earth's axis is tilted by 23.45o, therefore throughout the year declination angle varies between positive or negative magnitude. Declination angle for a particular day in a year can be calculated as (Page, 2018):

$$\delta = 23.45\,Sin\left[\left(\frac{360}{365}\right)(284+n)\right] \quad (8)$$

Hour angle ( ) for a particular instant or for a period of observation can be estimated as [43]:

$$\omega = (ST - 12)15^0 \quad (9)$$

Solar time (ST) or apparent solar time is a reckoning of the passage of time concerning the position of the sun in the sky. The relation between solar time and local time is established as (Duffie & Beckman, 2013; Page, 2018):

$$Standard\,time = ST - 4(L_{st} - L_{loc}) + E \quad (10)$$

where, E represents the equation of time (minutes) as:

$$E = 229.2(0.000075 + 0.001868\,Cos\,B - 0.032077\,Sin\,B - 0.014615\,Cos\,2B - 0.04089\,Sin\,2B) \quad (11)$$

The substitution of B, in Eq. (11). can be calculated through,

$$B = (n-1)\left(\frac{360}{365}\right) \quad (12)$$

Solar radiations loss due to end loss over a period of time can be calculated as:

$H_{loss} = \sum_{i=0}^{N} H_i * z_i$, when values have taken at regular intervals. (13)

$H_{loss} = \int_0^T H(t) * z(t)dt$, when analog time is considered. (14)

where,

Hi, H(t) = instantaneous value of DNI.(W/m2)

zi, z(t) = Instantaneous value of Aperture length of collector involved in end loss.

The end loss factor can be calculated for any parabolic trough with an arbitrary set of parameters given in Table 1 from the Eq. (1, 2, 3, 5, 6, 7, 8, 10, 11 and 12). The set of Eq. (1, 2, 3, 5, 6, 7, 9, 10, 11 and 12) can be used for parabolic trough placed horizontally on the surface and long axis oriented towards N-S direction. Moreover, instantaneous power loss, daily variation, daily average, annual variation and an annual average of energy loss due to end loss can be easily calculated using the appropriate beam radiation data arranged from credible data distribution centers and monitoring stations. Synthetic beam radiation data can also be generated for a particular location using computer algorithms.

In general, receiver length is kept equal to collector length in a parabolic trough. In order to collect the concentrated radiations that skip the interaction with the receiver due to oblique incidence of radiations, length of receiver can be extended with length, Δl as shown in Fig. 2. It would be advantageous in a smaller trough, as the end loss factor is much more significant than larger troughs.

3. Design of Experimental Setup

An indoor experimental set up is fabricated to emulate different angle of incidence over a parabolic trough and the length skipped by the ray after getting reflected from the trough is measured. Poly Trough - 1800 by NEPSOLAR is a commonly used commercial model of a parabolic trough for plant design, is taken as reference (Freeman et al., 2015). A miniature model is fabricated by scaling down the geometry.

Table 2- Specifications of Poly Trough - 1800 and Experimental Trough (NEP SOLAR AG, 2012)

Focal length and width of aperture are constructional feature and remains unchanged for any particular PTC. Incidence angle varies with time and respective to sun's position. Therefore, to design an experimental setup to evaluate the end losses, incidence angle is the only parameter that can be made variable.

Reflector substrate is constructed using aluminum sheet of 3 mm thickness. Metallized PET film, which is manufactured by depositing a thin layer of aluminum over the surface of PET substrate film to realize a bright metallic effect, is pasted over the Aluminum sheet, as shown in Fig. 3(a). The reflectivity of PET film is 95%, can be used up to 1200C for five years. The reflective tape has constant reflection over the visual range. Toy LASER lights of 650 nm with output power rated 5mW were chosen and arranged in array to create beam radiations. LASER has a collimated beam. Hence after getting reflected, it doesn't disperse as given in Fig. 3(b).

Fig. 3. (a) Metallized PET reflector film, (b) Schematic diagram of setup

Instead of a heat collecting element (HCE), transparent meter rulers are used to measuring the skipped length of the trough after the reflection of incident ray. Point of interception was identified with the center of the bright red spot on the ruler. 6 repeated observations of skipped length were recorded for angle of incidence with a step of 2o to improve measurement accuracy. A movable arm controls the incidence angle of LASER beam with a degree of freedom of 700. For performing the complete analysis of 900, trough support structure was designed to allow the adjustment in the inclination of the trough.

The indoor experiments were carried out from 20 -27 December 2019 at Solar Energy Lab, Energy Centre, Maulana Azad National Institute of Technology (MANIT), Bhopal, India. All the experiments were performed at night to ensure the location of LASER spots on the scale.

4. Experimental Uncertainty

Uncertainty plays a vital role in any experimentation. There are sources of error like systematic errors and random errors, which alter the outcome of measurements. Therefore, to get reliable measurement data, uncertainty analysis provides the range of possibly induced error in measurement. Uncertainty calculation of independent variables and calculated parameters are of much importance. The calculated uncertainties are given in Table 3. The total uncertainty in end loss factor (δEF) can occur from the skipped length, total length of trough and angle of incidence (Bevington et al., 1993; Taylor & Thompson, 1998). The uncertainty for the measurement in experimental setup should be minimum and can be estimated as (Chauhan et al., 2018):

$$\delta\mu = \sqrt{\left(\left(\frac{\partial\mu}{\partial z}.\delta z\right)^2 + \left(\frac{\partial\mu}{\partial l}.\delta l\right)^2 + \left(\delta\theta\ \frac{\cos\theta}{\sin\theta}\right)^2\right)} \quad (15)$$

Table 3- Uncertainties in variables and parameters

5. Results and discussions

Numerical simulation suggests that, as the angle of incidence increases, the skip length increases gradually in starting. However, a steeper upslope can be seen, which signifies the portion of trough providing end loss. All radiations at an angle greater than 84.8o skip the receiver tube due to the limited trough length. Hence, there is always critical angle for any arbitrary trough, after which all the radiations falling over the trough do not reflect on receiver. This critical incident angle holds much lower values for smaller troughs. Hence, compensation techniques must be employed in case of smaller troughs. Receiver extension is the most simple, effective and economical compensation method. It can be seen that, with receiver extension of 14 cms, end loss occurring for all the values of incidence angle below 40o can be eliminated. The discussed method of compensation can largely prevent end loss with the presented set of equations.

5.1 End loss simulation results

Analysis and calculations have been done for the mathematical model presented above and are presented in this section. The variables that directly affect the skip length are given in Table 2 and used in the analysis. Other variables that are used can be found in the abbreviation section in the last. Fig 4. shows the variation of declination for a year. It shows that by what angle the equatorial plane of the earth has been shifted w.r.t the line joining the center of earth and sun. Latitude (L), Hour angle (ω) and Declination angle (δ) jointly controls the angle of incidence (θ) for the case of parabolic trough.

Fig. 4. Declination angle (δ) over a year

Fig 5. shows the trend comparison between skip length (d/2), aperture of skip length (z) and aperture of total length of trough (z+y). The variation of the above variables has been noted w.r.t the angle of incidence (θ).

Fig. 5. Variation of trough length variables with θ

According to Eq. (1, 2, 3), the angle of incidence increases, the skip length increases gradually in starting, but a steeper upslope can be seen, which signifies the portion of trough providing end loss. All radiations falling over the surface of the trough at an angle greater than 84.8o

could not be collected at the receiver tube. Also, the aperture of skip length and total aperture length crossover point in Fig. 5 states the same phenomenon.

Fig. 6. Variation of end loss factor (%) with θ

The fraction of beam radiations skipping the receiver as the incidence angle of radiations falling over the surface increases is shown in Fig. 6. The incidence angle has been varied from 0o to 90o. The reason for the variation being non-linear is that the cosine effect and end loss effect are actions simultaneously. The cumulative percentage of radiation loss with the corresponding angle of incidence is shown in Table 4.

Table 4- Loss trend with angle of incidence

None of the radiation is reflected on the receiver for all the angles above 84.8o (Table 4). The first reason is the short length of receiver tube, which does not allow the reflected radiations to fall upon the receiver when the sun reaches lower altitudes. The second reason is long focal length of the parabolic trough. Longer the focal length of the trough, complete radiation loss will take place at lower angle of incidence.

Fig. 7. Impact of extended Receiver length on end loss due to incidence angle, θ

Radiation skipping the receiver after getting reflected from the collector surface results end loss. These skipping radiations can be collected by elongating the receiver tube. Fig. 7. shows the compensation of end loss (for a range of incidence angle) when receiver is extended with a certain length. It can be seen that, with receiver extension of 14 cms, end loss occurring for all the values of incidence angle below 40o can be eliminated. The length extension per degree of incidence angle is not constant as the dependency is non-linear in nature or the presented compensation technique, longitudinal tracking of focal line extremities is expensive and requires a reliable control system. Hence location-based length optimization of receiver tube is a better alternative.

5.2 Numerical simulation validation

Sun continuously ascends with time from sunrise till sunset in space fabric. The movement is well reflected in its azimuth and altitude angles when seen through a location on earth. For N-S orientation of trough altitude angle causes end loss. At the same time, azimuth is tracked with a single axis tracking mechanism. End loss model is developed to predict the end loss factor of any size of trough placed at any geographical location and orientation. Numerical model has also been validated with experimental values. The simulated and experimental results of end loss factor are presented in Fig. 8.

Fig. 8. Measured and Predicted skipped length with θ

End loss factor is 0% when the angle of incidence is 00 with respect to the normal surface (Fig. 8). End loss factor is limited to 5% when the incidence angle is lower than 280. Whereas for angles between 280 to 600, trough experience end loss between 5% and 15%. The end loss turns violent and increases exponentially above 600 incidence angles. However, trough length is a design feature and considers constant for a particular case. Still, the reflected radiations intercept the receiver, depending on the balance between the focus (x) and the trough length (l). Further, the predicted end loss factor exceeds 100% at an angle 84.80 due to the short trough length and practically impossible to measure it in experimentation.

Fig. 9. Error in skipped length measurement

The difference between predicted and experimental values of skipped trough length and end loss factor are in the range of -2.8 mm to 6.9 mm and -0.158 and 0.388, respectively, as shown

in Fig. 9. The predicted values of skipped length and end loss factor are also well matched with the experimental values. Therefore, prediction shows a fair agreement with the experimental observations.

Since the trend in error changing after 650, this is because of the high rate of skipped length and end loss factor with respect to the angle of incidence. It is an important design parameter and should always consider designing a parabolic trough field to limit the end loss.

6. Conclusion

The conclusions drawn based on end loss modeling and characteristics are:

i. End loss model covers a wide range of variables and is useful to analyze end loss variation with local time, solar time, latitude, dimensions of a trough and the angle of incidence of incoming beam radiations.

ii. End loss is dominantly dependent on the incidence angle and is non-linear. End loss factor is limited to 5% for values of incidence angle till 28%. For the angles between 28% and 60%, end loss factor was limited to 5% to 15%. End loss factor increases drastically for the angles over 60%.

iii. The difference between predicted and experimental values of skipped trough length and end loss factor are in the range of -2.8 mm to 6.9 mm and -0.158 and 0.388.

iv. Due to the limited length of trough, all radiations falling at higher inclination angles (near to 900) collected by the trough aperture skips the receiver. In such a case end loss factor will reach 100%, and for the present specimen, this phenomenon is occurring at 830.

v. Uncertainty measurement of skipped length was found to be 2.3 %, which is within the acceptable limit.

vi. Total uncertainty propagated in the calculation of end loss factor was 4.15 %. Therefore, the model is well validated with the experimental results obtained from the indoor setup.

It will make a more economically viable parabolic trough array setup for industrial applications. It could also enable readers to analyze end loss for non-standard sized troughs. Also, compensation of end loss using receiver extension can be personalized for different locations on the globe.

Acknowledgment

Authors are highly thankful to Maulana Azad National Institute of Technology -Bhopal (India) and Delhi Technological University, Delhi (India), for providing the necessary facilities for conducting this research work.

References

Agyekum, E. B., & Velkin, V. I. (2020). Optimization and techno-economic assessment of concentrated solar power (CSP) in South-Western Africa: A case study on Ghana. Sustainable Energy Technologies and Assessments, 40. https://doi.org/10.1016/j.seta.2020.100763

Al-Sulaiman, F. A., Zubair, M. I., Atif, M., Gandhidasan, P., Al-Dini, S. A., & Antar, M. A. (2015). Humidification dehumidification desalination system using parabolic trough solar air collector. Applied Thermal Engineering, 75. https://doi.org/10.1016/j.applthermaleng.2014.10.072

Andika, R., Kim, Y., Yoon, S. H., Kim, D. H., Choi, J. S., & Lee, M. (2017). Techno-economic assessment of technological improvements in thermal energy storage of concentrated solar power. Solar Energy, 157. https://doi.org/10.1016/j.solener.2017.08.064

Belgasim, B., Aldali, Y., Abdunnabi, M. J. R., Hashem, G., & Hossin, K. (2018). The potential of concentrating solar power (CSP) for electricity generation in Libya. In Renewable and Sustainable Energy Reviews (Vol. 90). https://doi.org/10.1016/j.rser.2018.03.045

Bellos, E., Tzivanidis, C., & Moghimi, M. A. (2019). Reducing the optical end losses of a linear Fresnel reflector using novel techniques. Solar Energy, 186. https://doi.org/10.1016/j.solener.2019.05.020

Bermejo, P., Pino, F. J., & Rosa, F. (2010). Solar absorption cooling plant in Seville. Solar Energy, 84(8). https://doi.org/10.1016/j.solener.2010.05.012

Bevington, P. R., Robinson, D. K., Blair, J. M., Mallinckrodt, A. J., & McKay, S. (1993). Data Reduction and Error Analysis for the Physical Sciences. Computers in Physics, 7(4). https://doi.org/10.1063/1.4823194

Brooks, M. J. (2005). Performance of a parabolic trough solar collector.

Chauhan, P. S., Kumar, A., Nuntadusit, C., & Banout, J. (2018). Thermal modeling and drying kinetics of bitter gourd flakes drying in modified greenhouse dryer. Renewable Energy, 118. https://doi.org/10.1016/j.renene.2017.11.069

Clark, J. A. (1982). An analysis of the technical and economic performance of a parabolic trough concentrator for solar industrial process heat application. International Journal of Heat and Mass Transfer, 25(9). https://doi.org/10.1016/0017-9310(82)90136-3

de Oliveira Siqueira, A. M., Gomes, P. E. N., Torrezani, L., Lucas, E. O., & da Cruz Pereira, G. M. (2014). Heat transfer analysis and modeling of a parabolic trough solar collector: An analysis. Energy Procedia, 57. https://doi.org/10.1016/j.egypro.2014.10.193

Duffie, J. A., & Beckman, W. A. (2013). Solar Engineering of Thermal Processes: Fourth Edition. In Solar Engineering of Thermal Processes: Fourth Edition. https://doi.org/10.1002/9781118671603

El-Kassaby, M. M. (1994). Prediction of optimum tilt angle for parabolic trough with the long axis in the north-south direction. International Journal of Solar Energy, 16(2). https://doi.org/10.1080/01425919408914269

El-Kassaby, M. M., & Hassab, M. A. (1995). Effect of parabolic trough solar collector orientation on its collection efficiency. International Journal of Solar Energy, 16(3). https://doi.org/10.1080/01425919508914275

El-Swify, M. E. (2001). Orientation and Tilt angle of parabolic trough solar concentrator at different latitudes. Journal of the Institution of Engineers (India), , 82(1), 10–18.

Freeman, J., Hellgardt, K., & Markides, C. N. (2015). An Assessment of Solar-Thermal Collector Designs for Small-Scale Combined Heating and Power Applications in the United Kingdom. Heat Transfer Engineering, 36(14–15). https://doi.org/10.1080/01457632.2015.995037

Gong, G., Huang, X., Wang, J., & Hao, M. (2010). An optimized model and test of the China's first high temperature parabolic trough solar receiver. Solar Energy, 84(12). https://doi.org/10.1016/j.solener.2010.08.003

Hafez, A. Z., Attia, A. M., Eltwab, H. S., ElKousy, A. O., Afifi, A. A., AbdElhamid, A. G., AbdElqader, A. N., Fateen, S. E. K., El-Metwally, K. A., Soliman, A., & Ismail, I. M. (2018).

Design analysis of solar parabolic trough thermal collectors. In Renewable and Sustainable Energy Reviews (Vol. 82). https://doi.org/10.1016/j.rser.2017.09.010

Hermann, W. A. (2006). Quantifying global exergy resources. Energy, 31(12). https://doi.org/10.1016/j.energy.2005.09.006

Islam, M. T., Huda, N., & Saidur, R. (2019). Current energy mix and techno-economic analysis of concentrating solar power (CSP) technologies in Malaysia. Renewable Energy, 140. https://doi.org/10.1016/j.renene.2019.03.107

Kalogirou, S. (1998). Use of parabolic trough solar energy collectors for sea-water desalination. Applied Energy, 60(2). https://doi.org/10.1016/S0306-2619(98)00018-X

Kalogirou, S. A. (2002). Parabolic trough collectors for industrial process heat in Cyprus. Energy, 27(9). https://doi.org/10.1016/S0360-5442(02)00018-X

Kalogirou, S. A. (2004). Solar thermal collectors and applications. In Progress in Energy and Combustion Science (Vol. 30, Issue 3). https://doi.org/10.1016/j.pecs.2004.02.001

Kalogirou, S. A. (2012). A detailed thermal model of a parabolic trough collector receiver. Energy, 48(1). https://doi.org/10.1016/j.energy.2012.06.023

Kumar, S., Agarwal, A., & Kumar, A. (2021). Financial viability assessment of concentrated solar power technologies under Indian climatic conditions. Sustainable Energy Technologies and Assessments, 43. https://doi.org/10.1016/j.seta.2020.100928

Lei, D., Li, Q., Wang, Z., Li, J., & Li, J. (2013). An experimental study of thermal characterization of parabolic trough receivers. Energy Conversion and Management, 69. https://doi.org/10.1016/j.enconman.2013.02.002

Li, M., Xu, C., Ji, X., Zhang, P., & Yu, Q. (2015). A new study on the end loss effect for parabolic trough solar collectors. Energy, 82. https://doi.org/10.1016/j.energy.2015.01.048

Lu, J., Ding, J., Yang, J., & Yang, X. (2013). Nonuniform heat transfer model and performance of parabolic trough solar receiver. Energy, 59. https://doi.org/10.1016/j.energy.2013.07.052

Luo, N., Yu, G., Hou, H. J., & Yang, Y. P. (2015). Dynamic Modeling and Simulation of Parabolic Trough Solar System. Energy Procedia, 69. https://doi.org/10.1016/j.egypro.2015.03.137

Ma, J., & Chang, Z. (2018). Understanding the effects of end-loss on linear Fresnelcollectors. IOP Conference Series: Earth and Environmental Science, 121(5). https://doi.org/10.1088/1755-1315/121/5/052052

Mohammadi, K., Khanmohammadi, S., Immonen, J., & Powell, K. (2021). Techno-economic analysis and environmental benefits of solar industrial process heating based on parabolic trough collectors. Sustainable Energy Technologies and Assessments, 47. https://doi.org/10.1016/j.seta.2021.101412

Morin, G., Dersch, J., Platzer, W., Eck, M., & Häberle, A. (2012). Comparison of Linear Fresnel and Parabolic Trough Collector power plants. Solar Energy, 86(1). https://doi.org/10.1016/j.solener.2011.06.020

NEP SOLAR AG. (2012, December). NEP-Solar-Polytrough1800_Datasheet. Https://Serv.Spf.Ch/Spftesting/Collectors/Pdfs/Scf1549en.Pdf.

Nolte, H. C., Bello-Ochende, T., & Meyer, J. P. (2015). Second law analysis and optimization of a parabolic trough receiver tube for direct steam generation. Heat and Mass Transfer /Waerme- Und Stoffuebertragung, 51(6). https://doi.org/10.1007/s00231-014-1465-3

Ouagued, M., Khellaf, A., & Loukarfi, L. (2013). Estimation of the temperature, heat gain and heat loss by solar parabolic trough collector under Algerian climate using different thermal oils. Energy Conversion and Management, 75. https://doi.org/10.1016/j.enconman.2013.06.011

Page, J. (2018). The role of solar-radiation climatology in the design of photovoltaic systems. In McEvoy's Handbook of Photovoltaics: Fundamentals and Applications. https://doi.org/10.1016/B978-0-12-809921-6.00016-1

Peng, S., Hong, H., Jin, H., & Zhang, Z. (2013). A new rotatable-axis tracking solar parabolic-trough collector for solar-hybrid coal-fired power plants. Solar Energy, 98(PC). https://doi.org/10.1016/j.solener.2013.09.039

Purohit, I., & Purohit, P. (2010). Techno-economic evaluation of concentrating solar power generation in India. Energy Policy, 38(6). https://doi.org/10.1016/j.enpol.2010.01.041

Salgado Conrado, L., Rodriguez-Pulido, A., & Calderón, G. (2017). Thermal performance of parabolic trough solar collectors. In Renewable and Sustainable Energy Reviews (Vol. 67). https://doi.org/10.1016/j.rser.2016.09.071

Sun, J., Liu, Q., & Hong, H. (2015). Numerical study of parabolic-trough direct steam generation loop in recirculation mode: Characteristics, performance and general operation strategy. Energy Conversion and Management, 96. https://doi.org/10.1016/j.enconman.2015.02.080

Tagle-Salazar, P. D., Nigam, K. D. P., & Rivera-Solorio, C. I. (2020). Parabolic trough solar collectors: A general overview of technology, industrial applications, energy market, modeling, and standards. In Green Processing and Synthesis (Vol. 9, Issue 1). https://doi.org/10.1515/gps-2020-0059

Taylor, J. R., & Thompson, W. (1998). An Introduction to Error Analysis: The Study of Uncertainties in Physical Measurements. Physics Today, 51(1). https://doi.org/10.1063/1.882103

Tiwari, G. N., & Tiwari, A. (2017). Handbook of solar energy. Singapore. Springer.

Valizade, M., Heyhat, M. M., & Maerefat, M. (2020). Experimental study of the thermal behavior of direct absorption parabolic trough collector by applying copper metal foam as volumetric solar absorption. Renewable Energy, 145. https://doi.org/10.1016/j.renene.2019.05.112

Xu, C., Chen, Z., Li, M., Zhang, P., Ji, X., Luo, X., & Liu, J. (2014). Research on the compensation of the end loss effect for parabolic trough solar collectors. Applied Energy, 115. https://doi.org/10.1016/j.apenergy.2013.11.003

Xu, E., Zhao, D., Xu, H., Li, S., Zhang, Z., Wang, Z., & Wang, Z. (2015). The Badaling 1MW Parabolic Trough Solar Thermal Power Pilot Plant. Energy Procedia, 69. https://doi.org/10.1016/j.egypro.2015.03.096

Xu, R., & Wiesner, T. F. (2015). Closed-form modeling of direct steam generation in a parabolic trough solar receiver. Energy, 79(C). https://doi.org/10.1016/j.energy.2014.11.004

Zhu, S., Yu, G., Ma, Y., Cheng, Y., Wang, Y., Yu, S., Wu, Z., Dai, W., & Luo, E. (2019). A free-piston Stirling generator integrated with a parabolic trough collector for thermal-to-electric conversion of solar energy. Applied Energy, 242. https://doi.org/10.1016/j.apenergy.2019.03.169

Zou, B., Dong, J., Yao, Y., & Jiang, Y. (2016). An experimental investigation on a small-sized parabolic trough solar collector for water heating in cold areas. Applied Energy, 163. https://doi.org/10.1016/j.apenergy.2015.10.186

Zou, B., Yang, H., Yao, Y., & Jiang, Y. (2017). A detailed study on the effects of sunshape and incident angle on the optical performance of parabolic trough solar collectors. Applied Thermal Engineering, 126. https://doi.org/10.1016/j.applthermaleng.2017.07.149

Rawani, A. T. W. A. R. I., S. P. Sharma, and K. D. P. Singh. "Comparative performance analysis of different twisted tape inserts in the absorber tube of parabolic trough collector." International Journal of Mechanical and Production Engineering Research and Development 8.1 (2018): 643-656.

Senthil, R., and A. P. Nishanth. "Optical and thermal performance analysis of solar parabolic concentrator." International Journal of Mechanical and Production Engineering Research and Development 7.5 (2017): 367-374.

Senthil, R. A. M. A. L. I. N. G. A. M., M. U. K. U. N. D. Gupta, and C. H. I. N. M. A. Y. A. Rath. "Parametric analysis of a concentrated solar receiver with Scheffler reflector." International Journal of Mechanical and Production Engineering Research and Development 7.5 (2017): 261-268.

Senthil, R. "Effect of secondary reflector on thermal performance of linear fresnel concentrated solar collector." International Journal of Mechanical and Production Engineering Research and Development 8.4 (2018).

Kumar, M., B. Veerabhadra Reddy, and P. Venkateshwar Reddy. "Experimental Comparison of Solar Paraboloid Collector with and without Mirror in Aluminum Foil as Reflectors." International Journal of Mechanical and Production Engineering Research and Development (IJMPERD) 8.2 (2018): 1117-1124.

Parveen, M., and O. H. Mohideen. "A Study on Financial Performance of Pharmaceutical Company Using Five Power Analyses." International Journal of Business Management & Research (IJBMR) 1.4 (2014): 45-50.

Annexure:

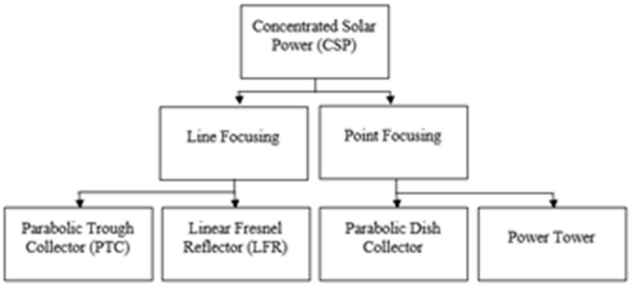

FIGURE 1. Classification of CSP

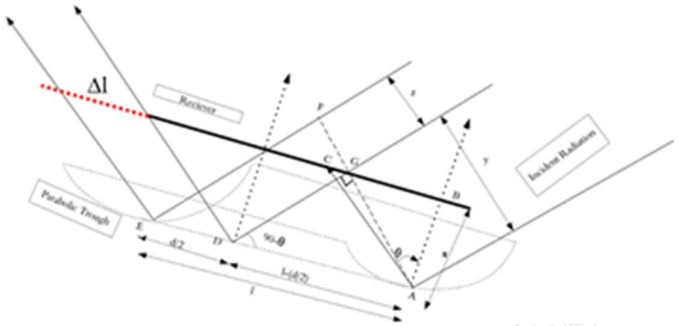

FIGURE 2. Schematic diagram for parabolic trough

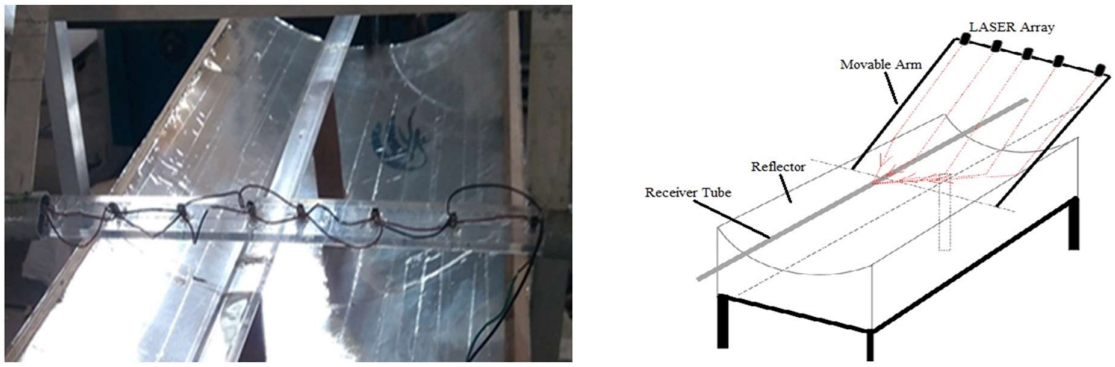

(a) (b)

FIGURE 3. (a) Metallized PET reflector film, (b) Schematic diagram of setup

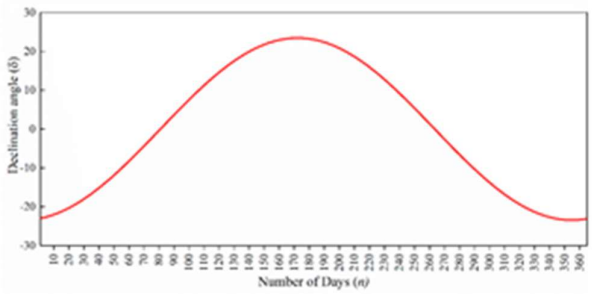

FIGURE 4. Declination angle (δ) over a year

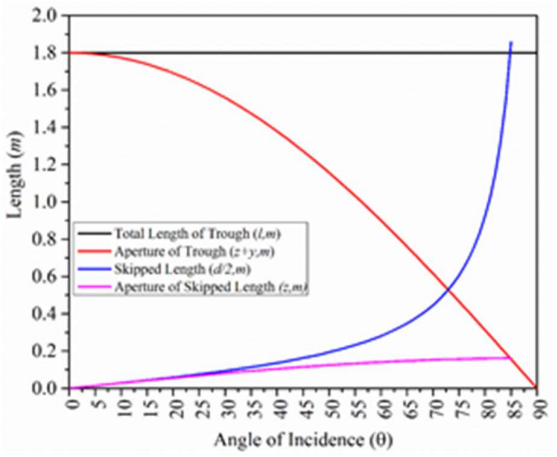

FIGURE 5. Variation of trough length variables with θ

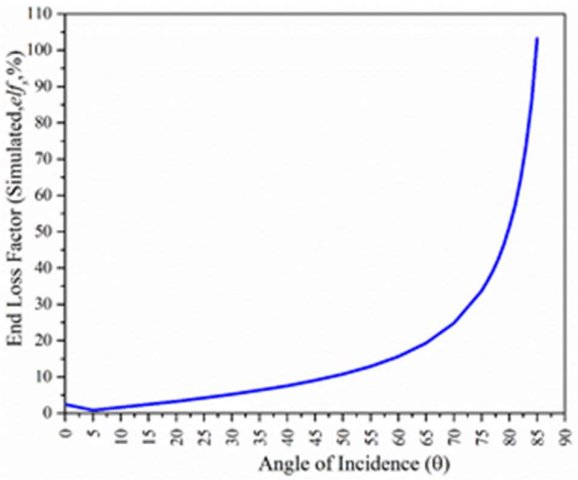

FIGURE 6. Variation of end loss factor (%) with θ

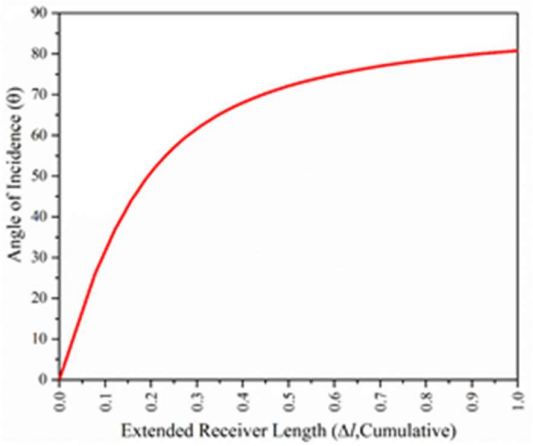

FIGURE 7. Impact of extended Receiver length on end loss due to incidence angle, θ

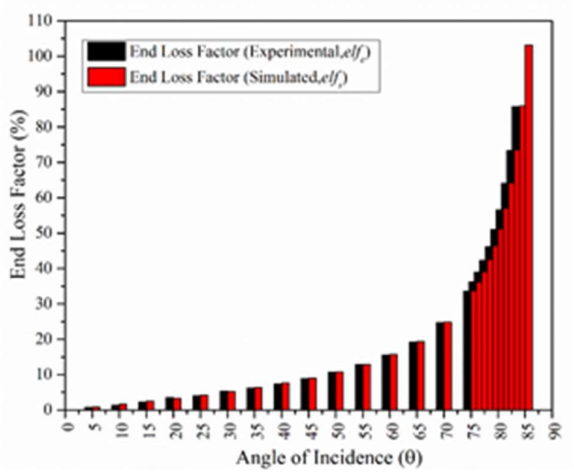

FIGURE 8. Measured and Predicted skipped length with θ

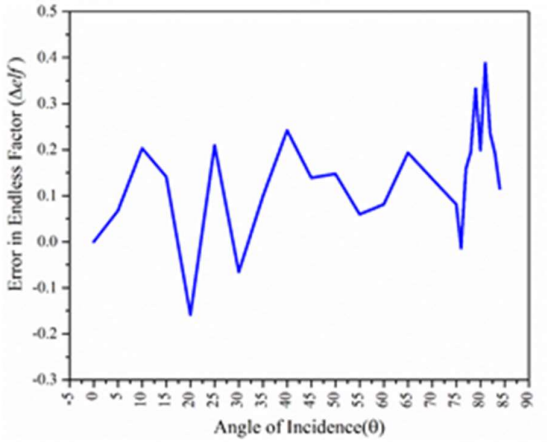

FIGURE 9. Error in skipped length measurement

Table 1- Characteristics of quantities affecting end loss

S. No.	Symbol	Parameter	Dependency	Range	Reference
1.	θ	Angle of incidence	f (L, δ, a_s, β, ω)	$-90^0 \le \theta \le 90^0$	Ouagued et al., 2013
2.	L	local latitude	independent	90^0 N ≤ L ≤ 90^0 S	Ouagued et al., 2013
3.	δ	declination angle	f(n)	$-23.45^0 \le \delta \le 23.45^0$	Ouagued et al., 2013
4.	a_s	surface azimuth angle	f(a_f)	0^0 to 360^0 due south	Page., 2012
5.	β	surface tilt angle from horizontal surface	independent	$0^0 \le \beta \le 90^0$	Ouagued et al., 2013

6.	ω	hour angle	f(ST)	0 to 24 hours	Mghouchi et al., 2016
7.	θ_z	solar zenith angle	independent	$0^0 \leq \theta_z \leq 90^0$	Ouagued et al., 2013
8.	n	day of the year	independent	$1 \leq n \leq 365$	Page., 2012
9.	w	aperture width of the trough	Depends upon design and trough profile	NA	

Table 2- Specifications of Poly Trough - 1800 and Experimental Trough [Dataset]

S.No	Specification	Poly Trough - 1800	Experimental Model
1.	Aperture Area, A_{ap}	36.9 m^2	0.94 m^2
2.	Length, l	20.9 m	1.8 m
3.	Width, w	1.845 m	0.52 m
4.	Focal Length, x	0.65 m	0.1625 m
5.	Rim Angle, r	71^0	71.6^0
6.	Concentration ratio (geometric), C_{geo}	54	-----

(Source: http://www.nep-solar.com/wp-content/uploads/2013/11/NEP-Solar-Polytrough1800_Datasheet.pdf)

Table 3- Uncertainties in variables and parameters

S.No.	Quantity	Uncertainty
1.	Skipped Length (d/2)	± 0.002 m
2.	Angle of Incidence (θ)	± 1^0
3.	Length of Trough (l)	± 0.001 m
4.	Solar Radiation (H)	± 10 W/m^2
5.	Aperture of skipped length (z)	2.3%
6.	Aperture of length of trough (z+y)	1.86%
7.	End loss factor (μ)	4.15%

Table 4- Loss trend with angle of incidence

Angle of Incidence, θ	**0°**	**10°**	**20°**	**30°**	**40°**	**50°**	**60°**	**70°**	**80°**	**84.8°**	**90°**
End loss Factor (%)	0 %	1.6 %	3.28 %	5.21 %	7.57 %	10.75 %	15.63 %	24.80 %	51.19 %	100 %	NA